



CSIC

CONSEJO SUPERIOR DE INVESTIGACIONES CIENTÍFICAS



EXCELENCIA
MARÍA
DE MAEZTU



OPTIMIZATION OF A MICROWAVE POLARIMETER FOR ASTRONOMY WITH OPTICAL CORRELATION AND DETECTION

G. Pascual-Cisneros, F.J. Casas, P. Vielva



INTRODUCTION

- Nowadays, CMB faint B-mode detection is one of the main cosmological objectives.
- In order to measure the faint B-mode pattern, experiments with increasing sensitivity are needed.
- Foregrounds characterization plays a main role due to the faint signal of the B-modes. So, coordinated multifrequency analysis should be made

INTRODUCTION: DIRECT IMAGE VS INTERFEROMETRY

- On CMB experiments Direct image detectors is the main approach but sensitivity is limited by the focal plane size.
- On the other hand, Interferometric designs are not space limited but low frequency interferometers can not afford the required high number of detectors, due to limitations in phase controlling and routing of a high number of microwave signals.
- Two different technological approaches can be used to solve this issue: digital correlators based on FPGAs and electro-optical ones based on MZM modulators.

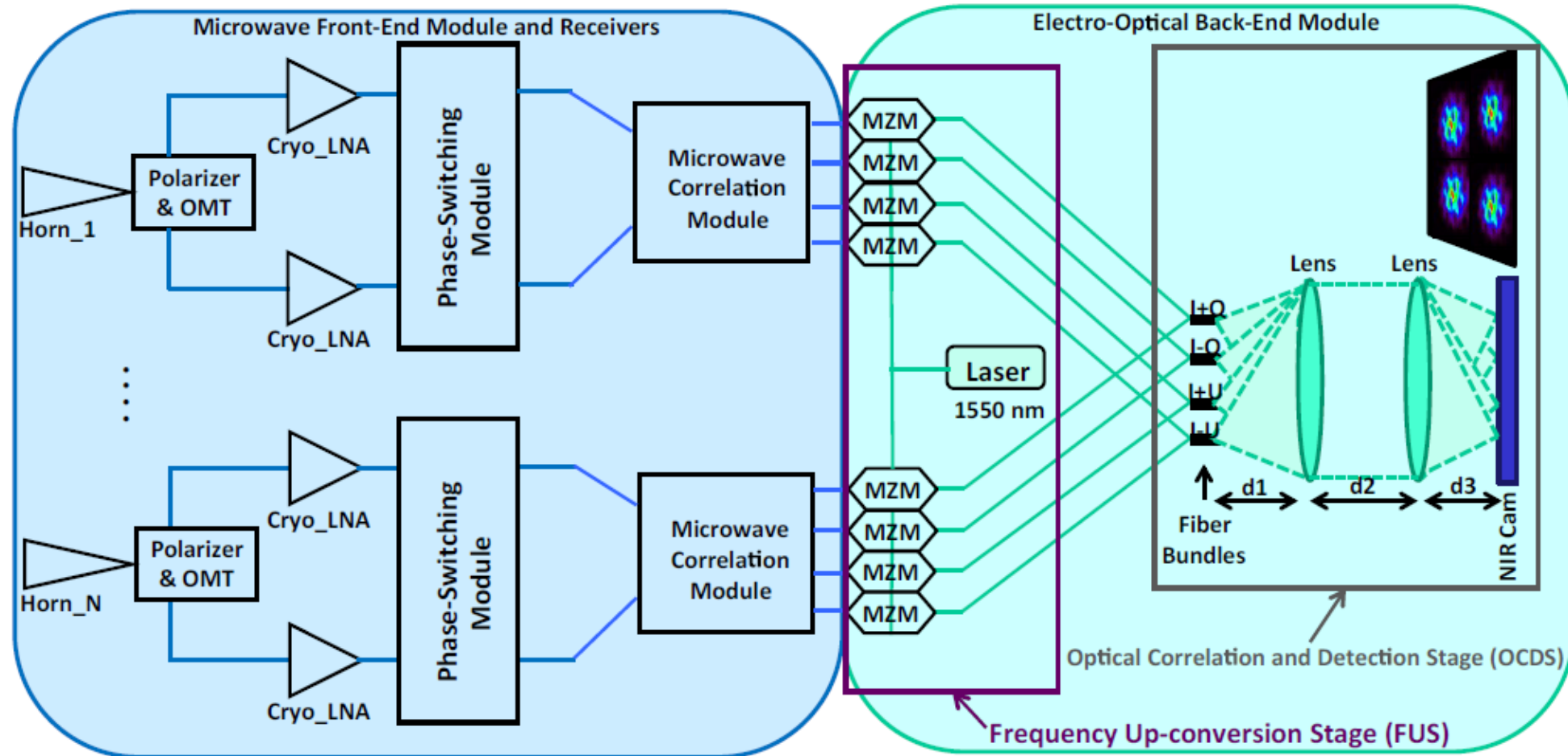
INTRODUCTION: FPGA VS ELECTRO-OPTIC SCHEME

- FPGAs can be used to implement a Michelson Interferometer but the required number of cards will grow as the number of baselines:

$$N_{FPGA} = \frac{N(N - 1)}{2}$$

- Using electro-optic modulators and a simple optical configurations, we can develop a Fizeau interferometer which will produce a final synthesized image.

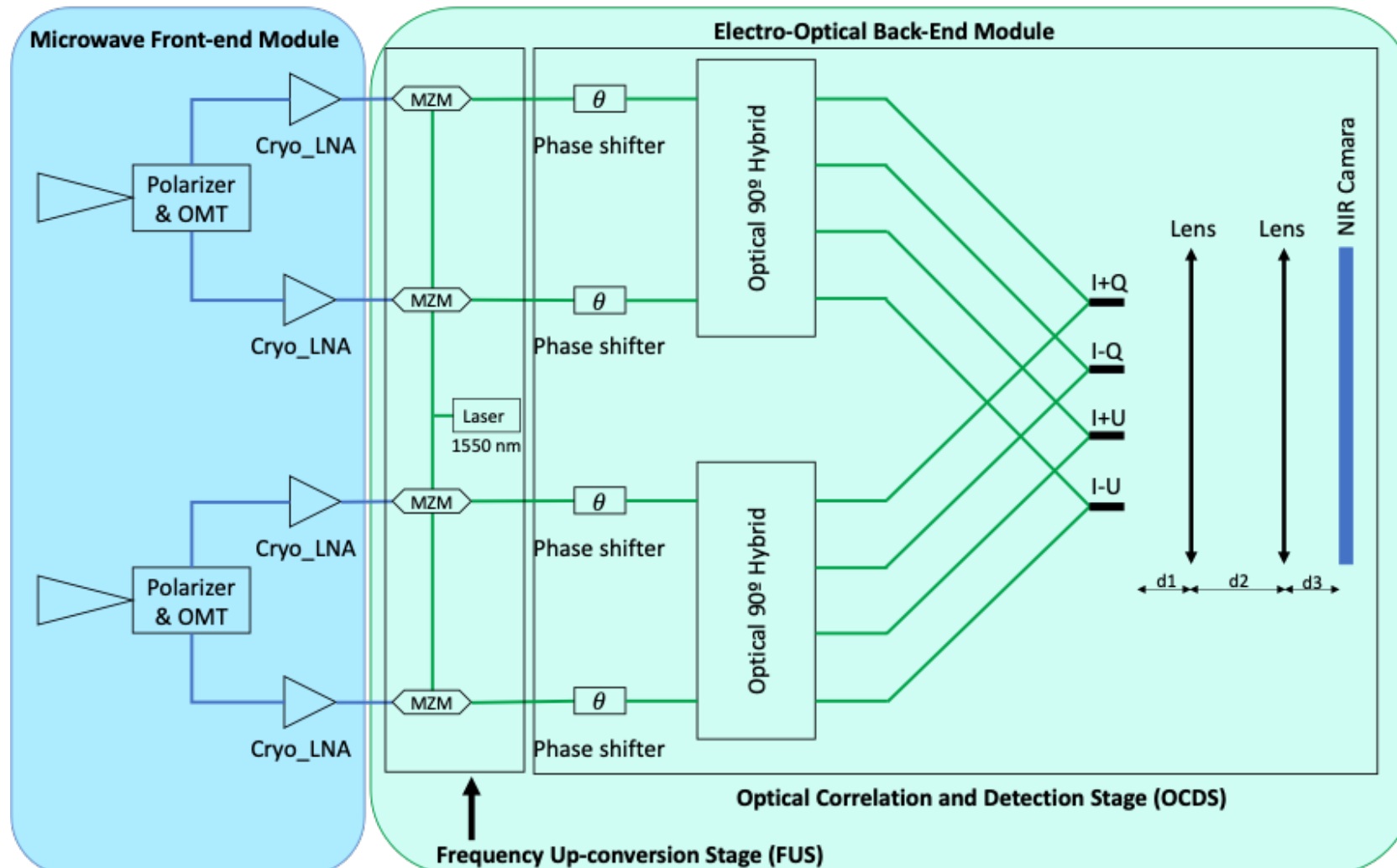
SYNTHESIZED IMAGE POLARIMETER IDEA



Casas, F.J.; Ortiz, D.; Aja, B.; de la Fuente, L.; Artal, E.; Ruiz, R.; Mirapeix, J.M. A Microwave Polarimeter Demonstrator for Astronomy with Near-Infra-Red Up-Conversion for Optical Correlation and Detection. *Sensors* **2019**, *19*, 1870.

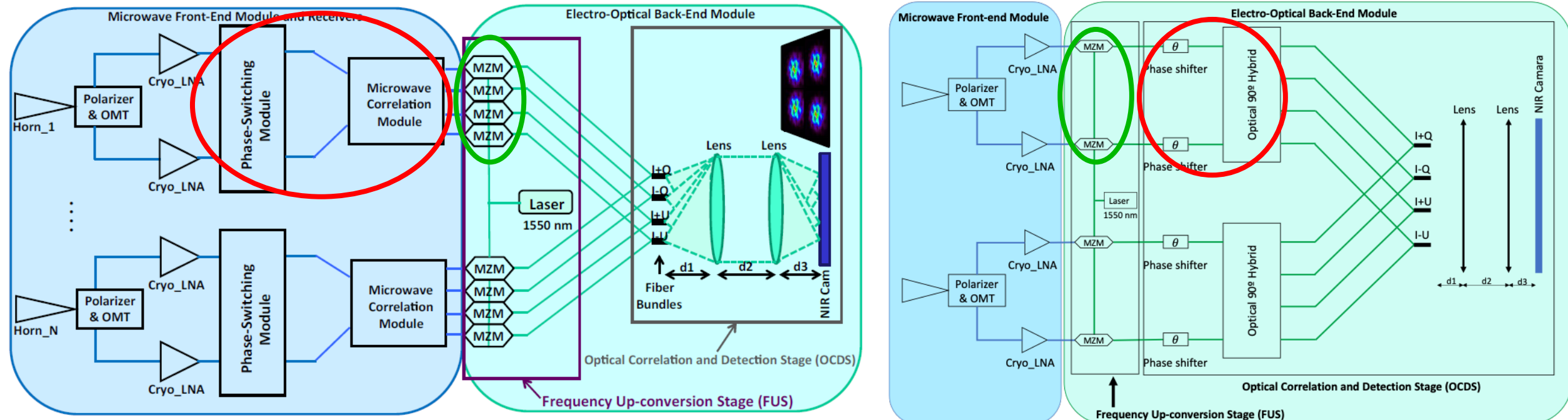
<https://doi.org/10.3390/s19081870>

NEW POLARIMETER SCHEME



OLD VS NEW

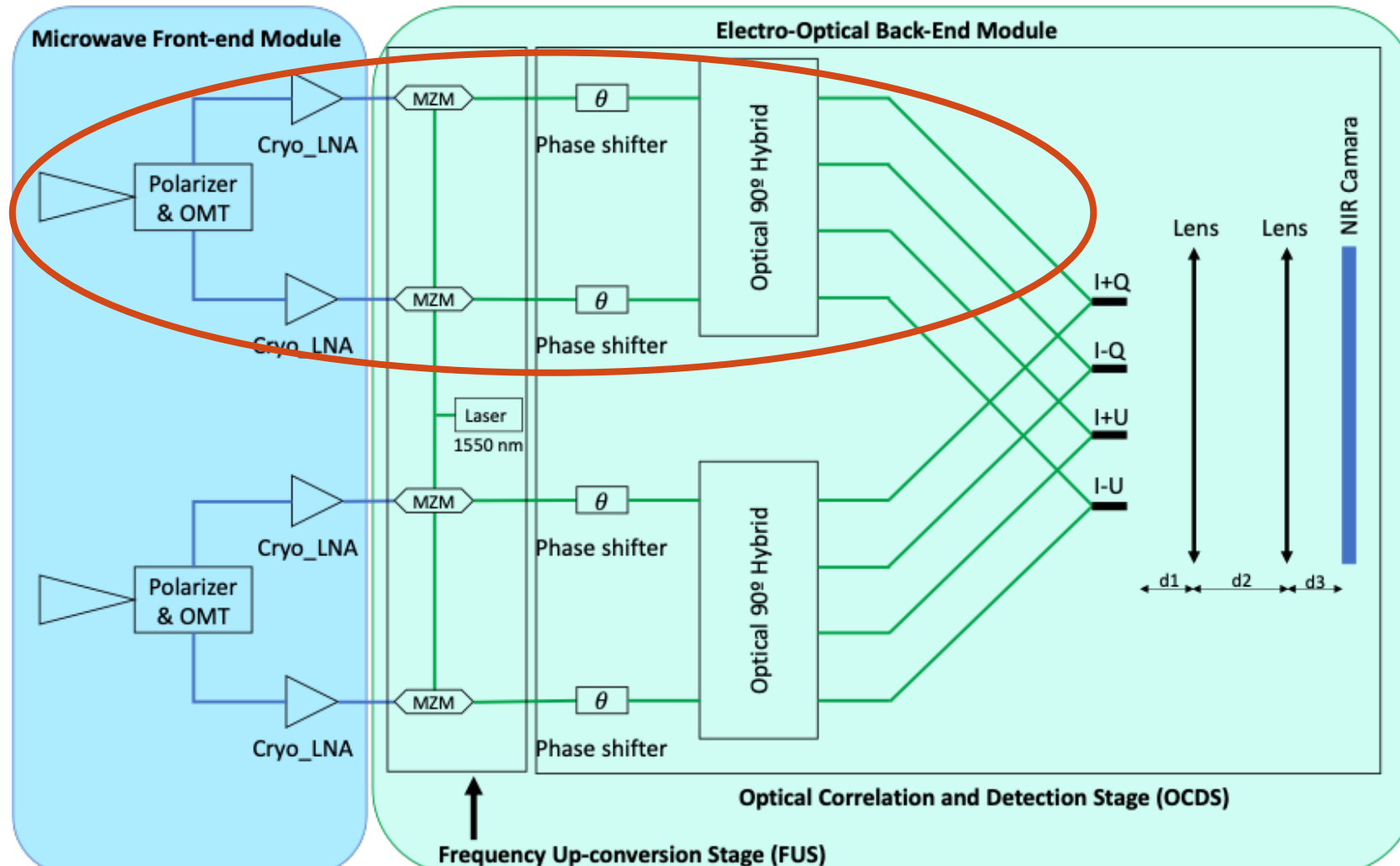
- The main change is that the microwave correlation part in the Old Scheme has been moved to the optical part.



OLD VS NEW

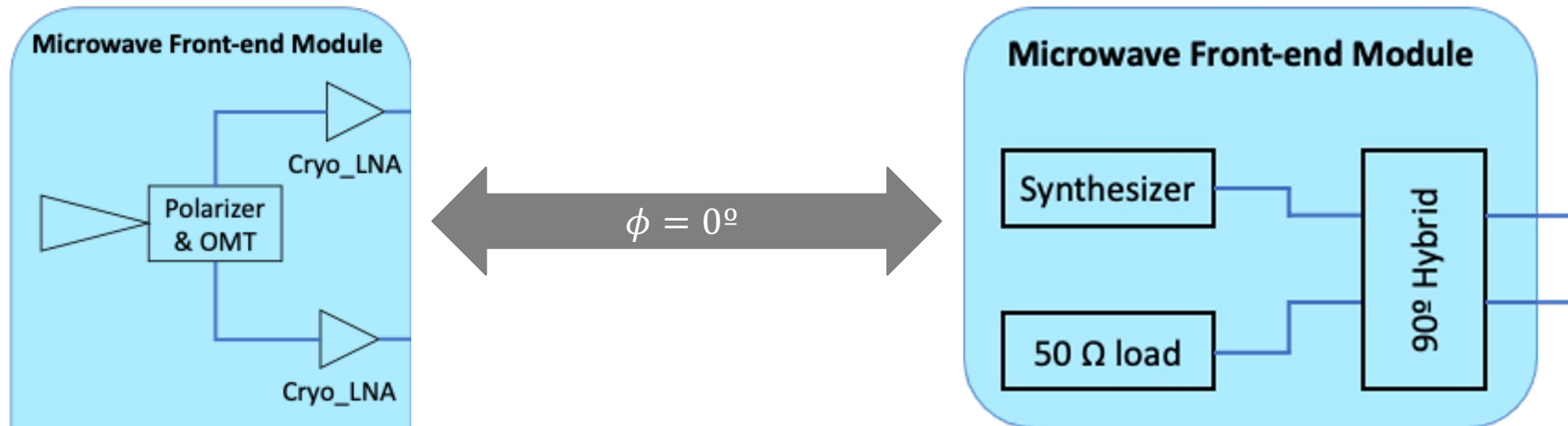
- The main change is that the microwave correlation part in the Old Scheme has been moved to the optical part.
- This allows to reduce the number of MZM by a factor of 2, allowing a noticeable reduction in cost, volume, weight and power consumption
- Another advantage of the new model is that it can be integrated on a InP chip using Photonic Integrated Technology (PICs)

LABORATORY DEMONSTRATOR: DIRECT DETECTION



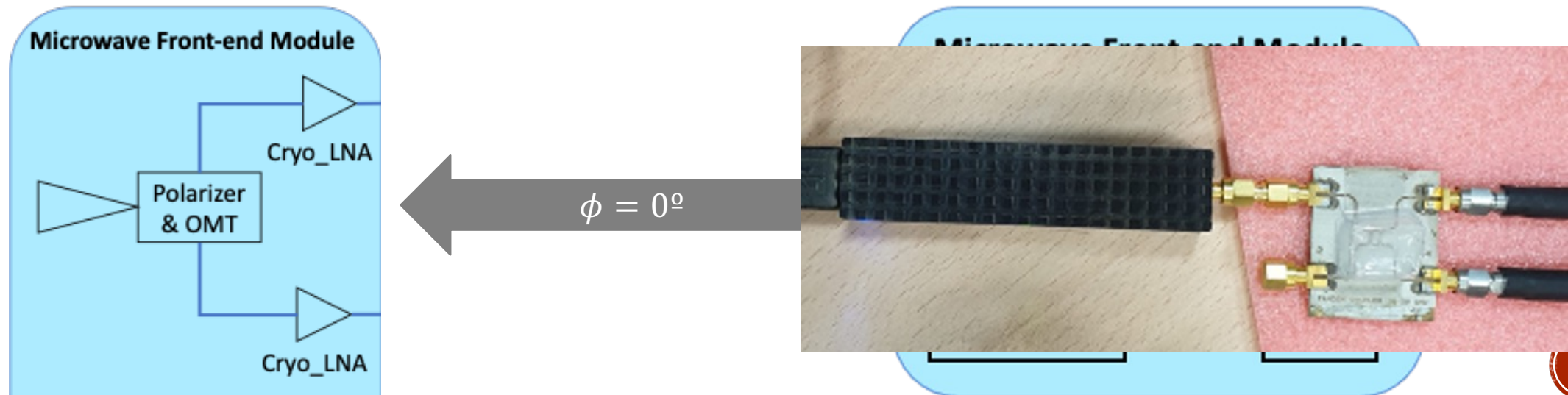
LABORATORY DEMONSTRATOR: FRONT-END

- Instead of using a microwave front-end composed by a horn antenna a polariser and a OMT, a mono-frequency signal of 10 GHz, produced by a frequency synthesizer, is connected to a 90° hybrid with the other input connected to a 50 Ω load.
- This scheme produce 2 signals equivalent to the ones produced by the original scheme if the input signal polarization angle is 0°



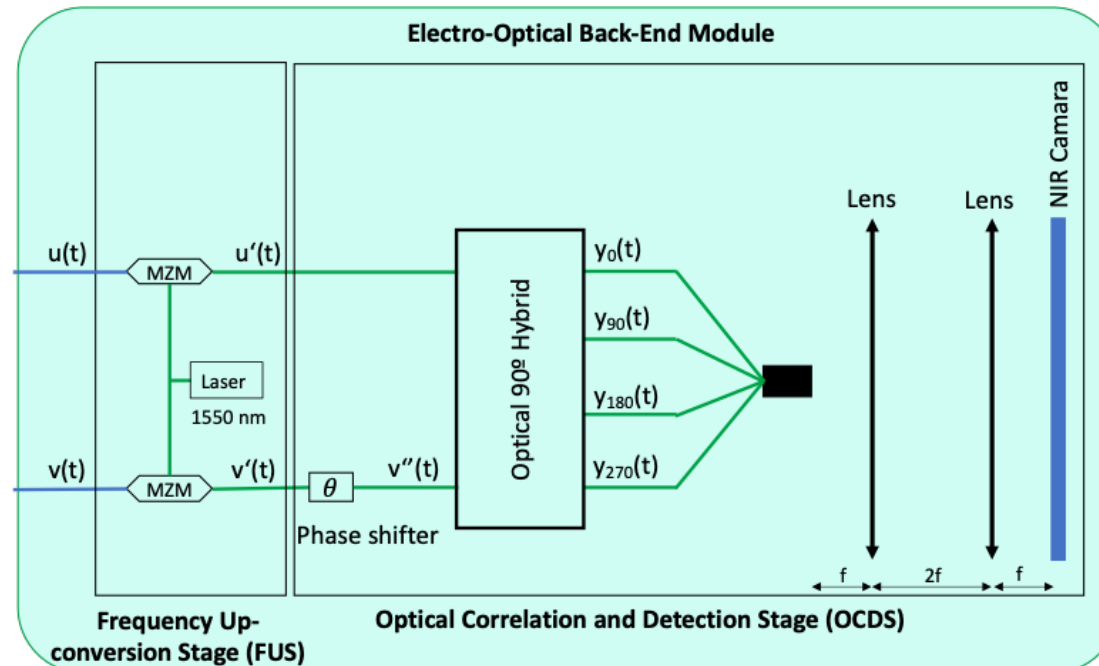
LABORATORY DEMONSTRATOR: FRONT-END

- Instead of using a microwave front-end composed by a horn antenna a polariser and a OMT, a mono-frequency signal of 10 GHz, produced by a frequency synthesizer, is connected to a 90° hybrid with the other input connected to a 50 Ω load.
- This scheme produce 2 signals equivalent to the ones produced by the original scheme if the input signal polarization angle is 0°

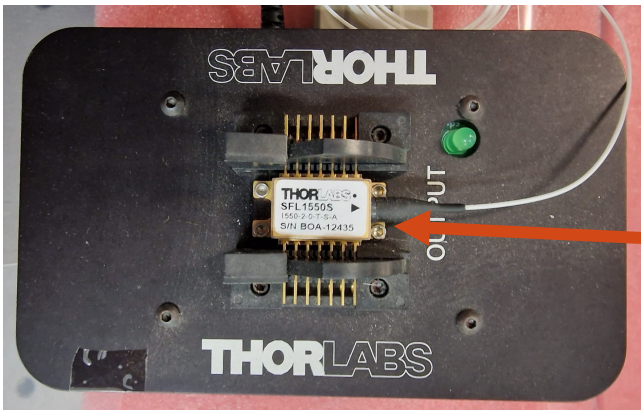
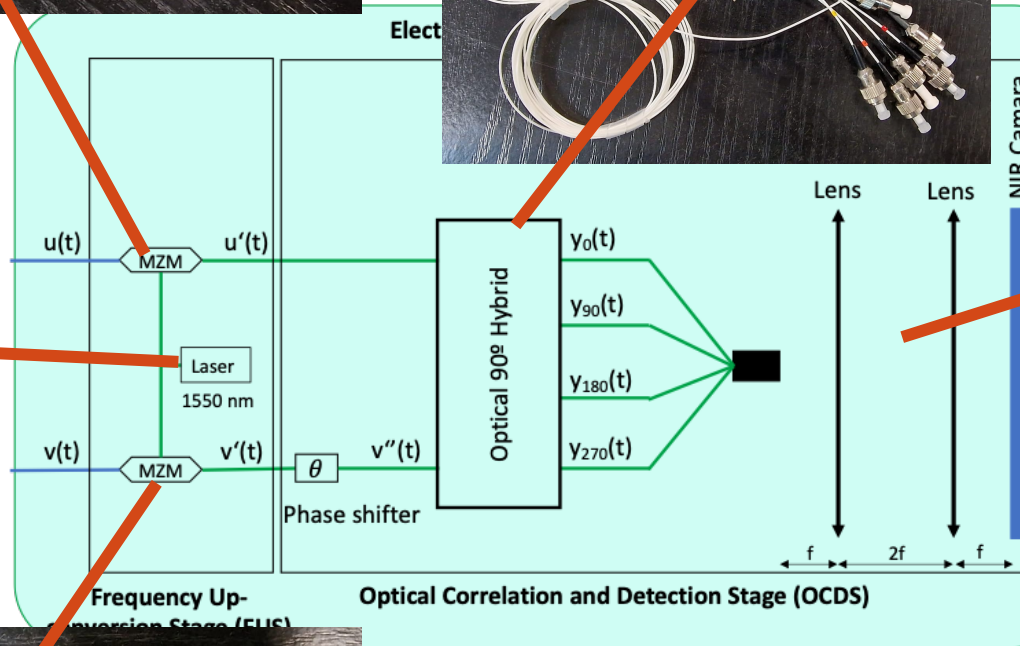
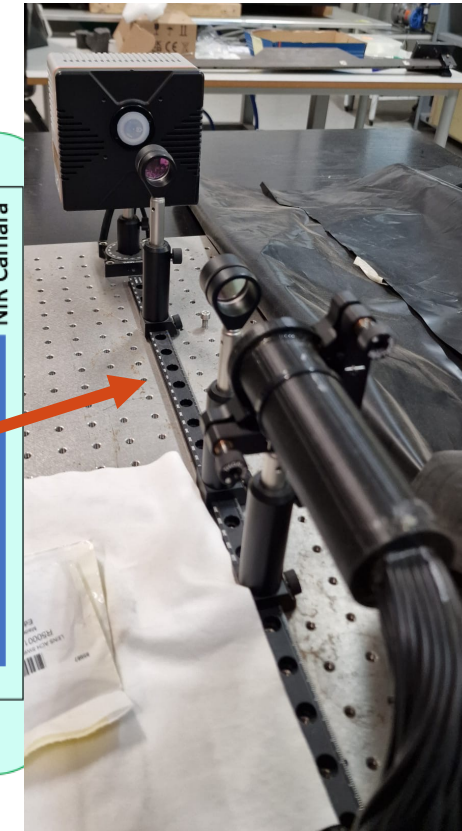
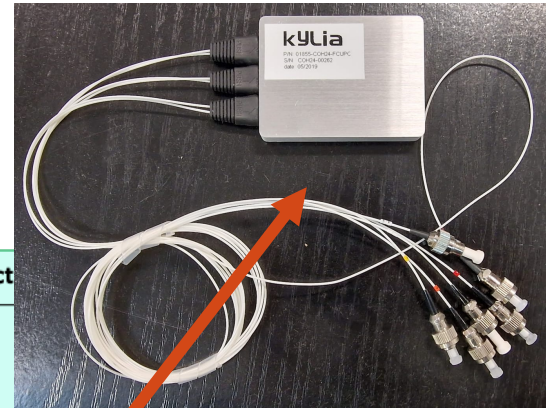
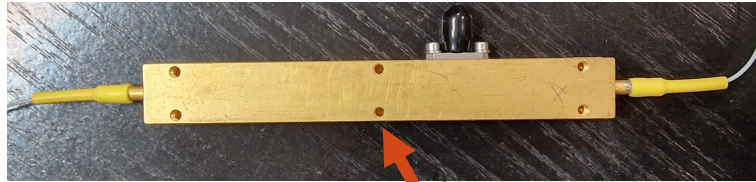


LABORATORY DEMONSTRATOR: BACK-END

- The Back-End module is in charge of obtaining the in phase and quadrature combinations of the 2 optically upconverted input signals giving 4 outputs proportional to the combinations of I, Q and U stokes parameters.
- The phase shifter modulates the phase difference between the signals (u' and v') allowing to see all the stokes combinations on every single output y_i .

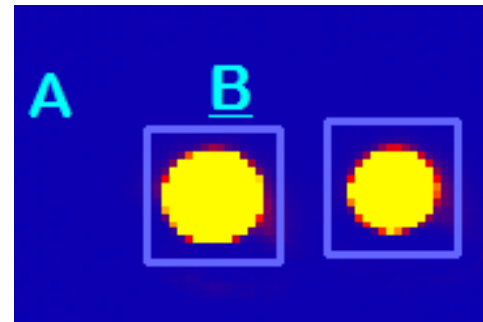


LABORATORY DEMONSTRATOR: BACK-END



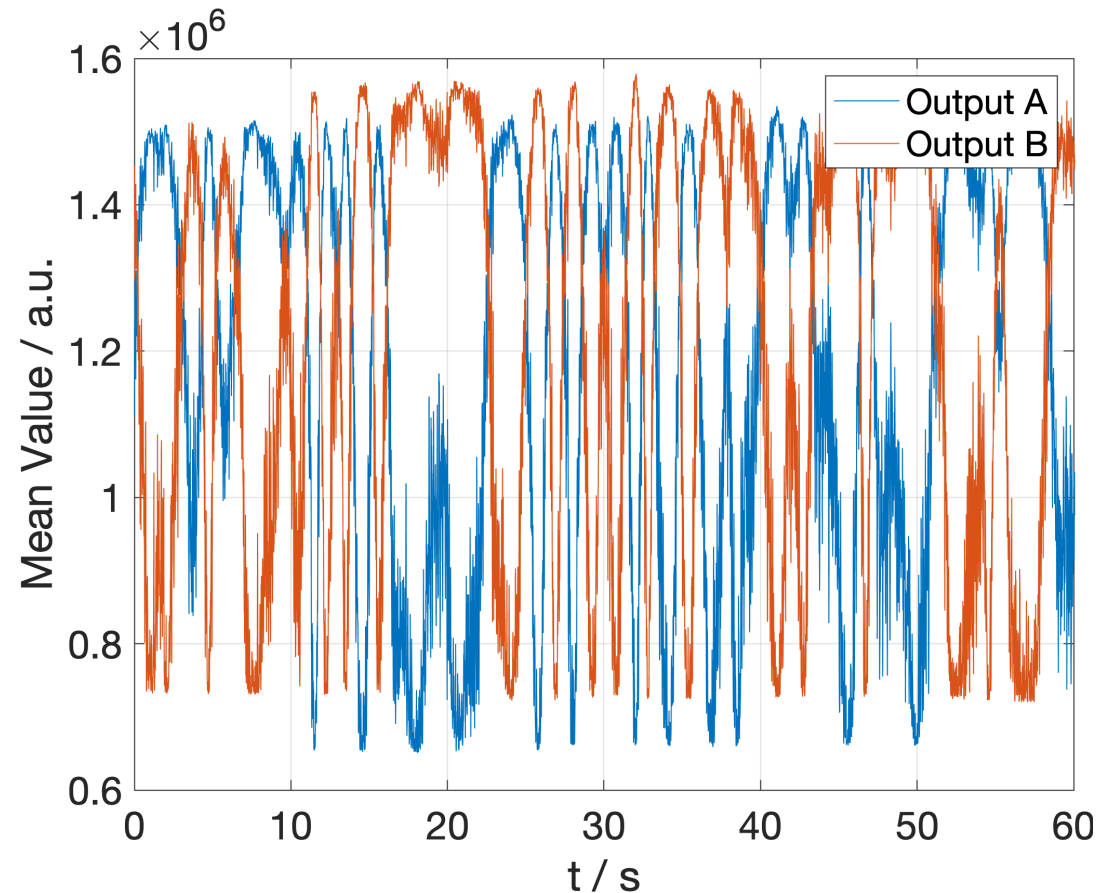
DEMONSTRATOR RESULTS

- In the first test, only 2 out of the 4 outputs are measured with no external phase modulation.
- Measurements are obtained by taking the mean power on the light blue boxes around the beams

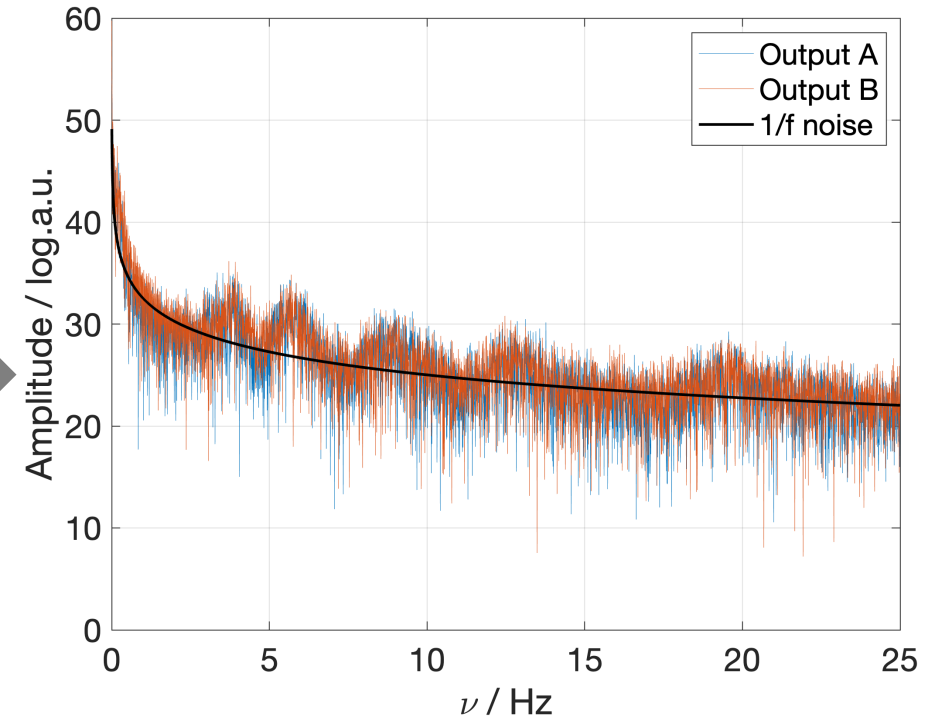
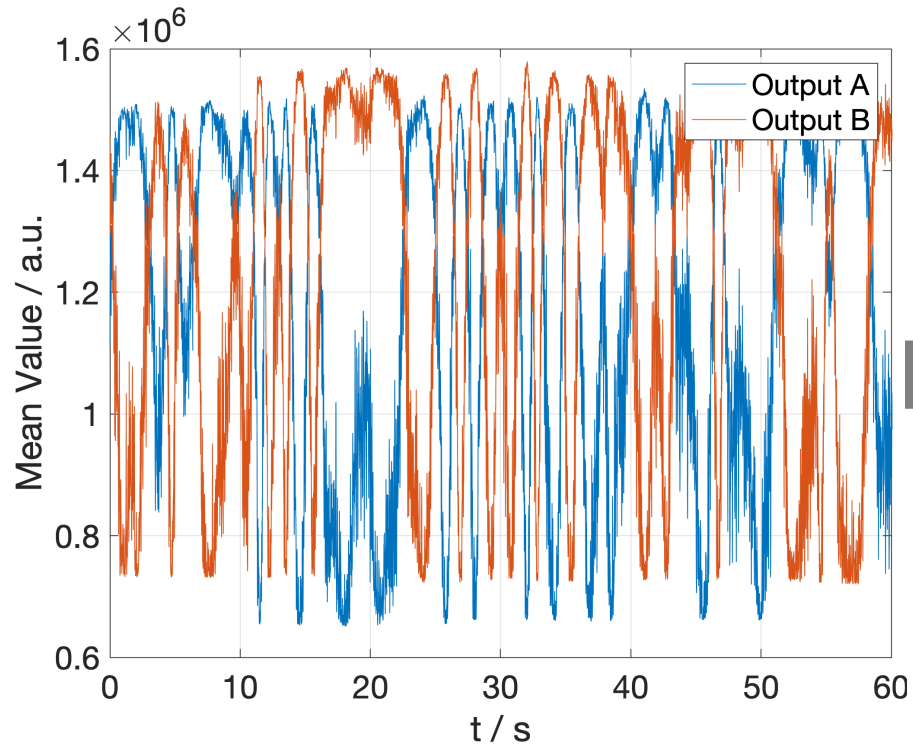


DEMONSTRATOR RESULTS

- In the first test, only 2 out of the 4 outputs are measured with no external phase modulation.



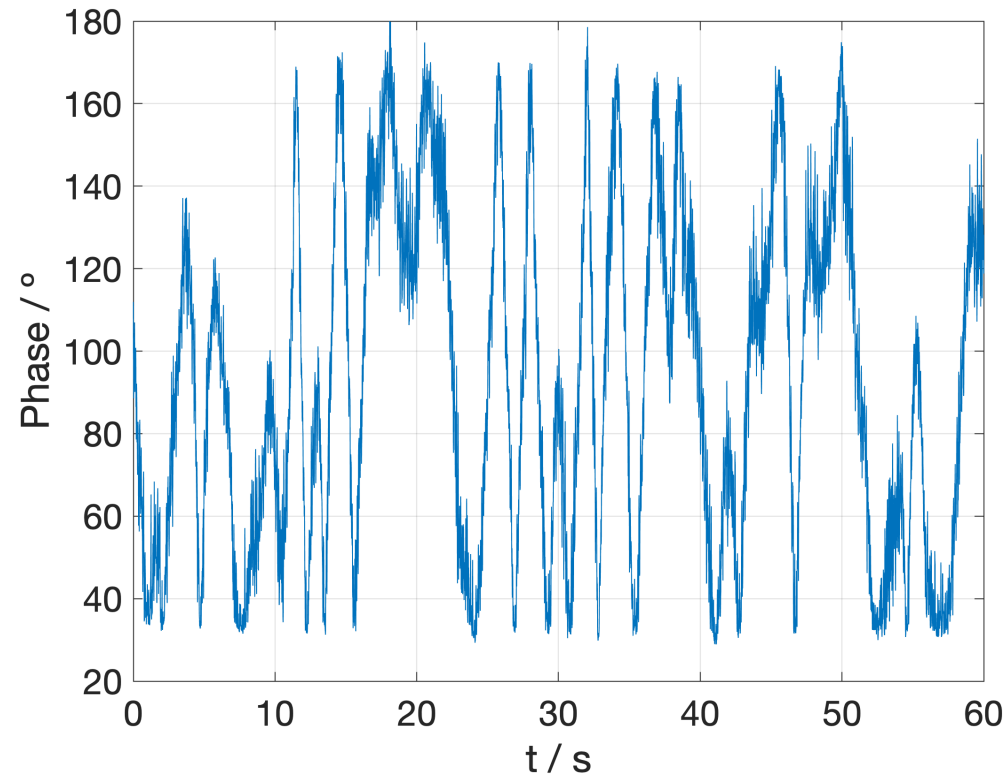
1/F LIKE NOISE



- As the frequency range of this noisy signal is similar to the one provided by our optical phase shifters it was not possible to perform a complete functional test of the polarimeter. Instead of this, a theoretical performance analysis were done by modelling and simulation of an equivalent system with much higher modulation frequency.

1/F LIKE NOISE

- This noise is produced by changes on the optical path in the system generated by external agents as vibrations, temperature and atmospheric pressure or mismatches on fiber junctions.
- It can be converted to phase fluctuations.



THEORETICAL MODEL

- Lets develop a simple theoretical model to see if fast modulation is enough to calibrate the reported random noise.

- Input signal: $y(t) = Ae^{i2\pi f_m t}$,

- Front-End module output signals:

$$\begin{aligned} u(t) &= (A_x + iA_y)e^{i2\pi f_m t} \\ v(t) &= (A_y + iA_x)e^{i2\pi f_m t} \end{aligned}$$

- with

$$\begin{aligned} A_x &= A \cos \phi \\ A_y &= A \sin \phi \end{aligned}$$

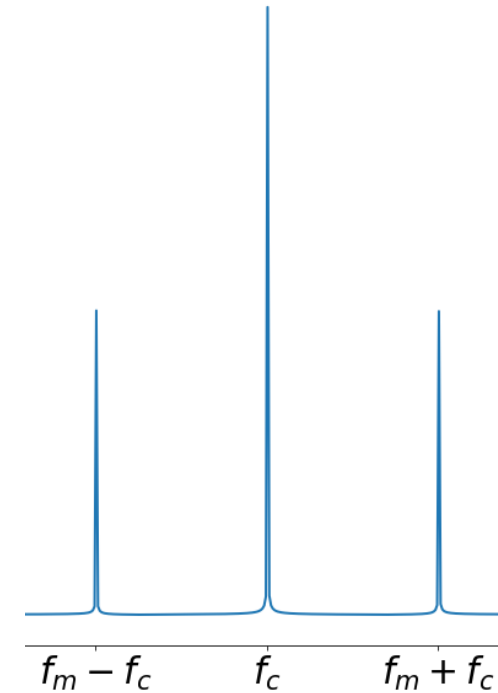
- Therefore:

$$\begin{aligned} u(t) &= Ae^{i2\pi f_m t} e^{i\phi} \\ v(t) &= Ae^{i2\pi f_m t} i e^{-i\phi} \end{aligned}$$

THEORETICAL MODEL

- We used the next expression to model MZM behaviour:

$$u'(t) = u(t) \frac{e^{i2\pi f_c t} + e^{-i2\pi f_c t}}{2} + k e^{i2\pi f_c t}$$

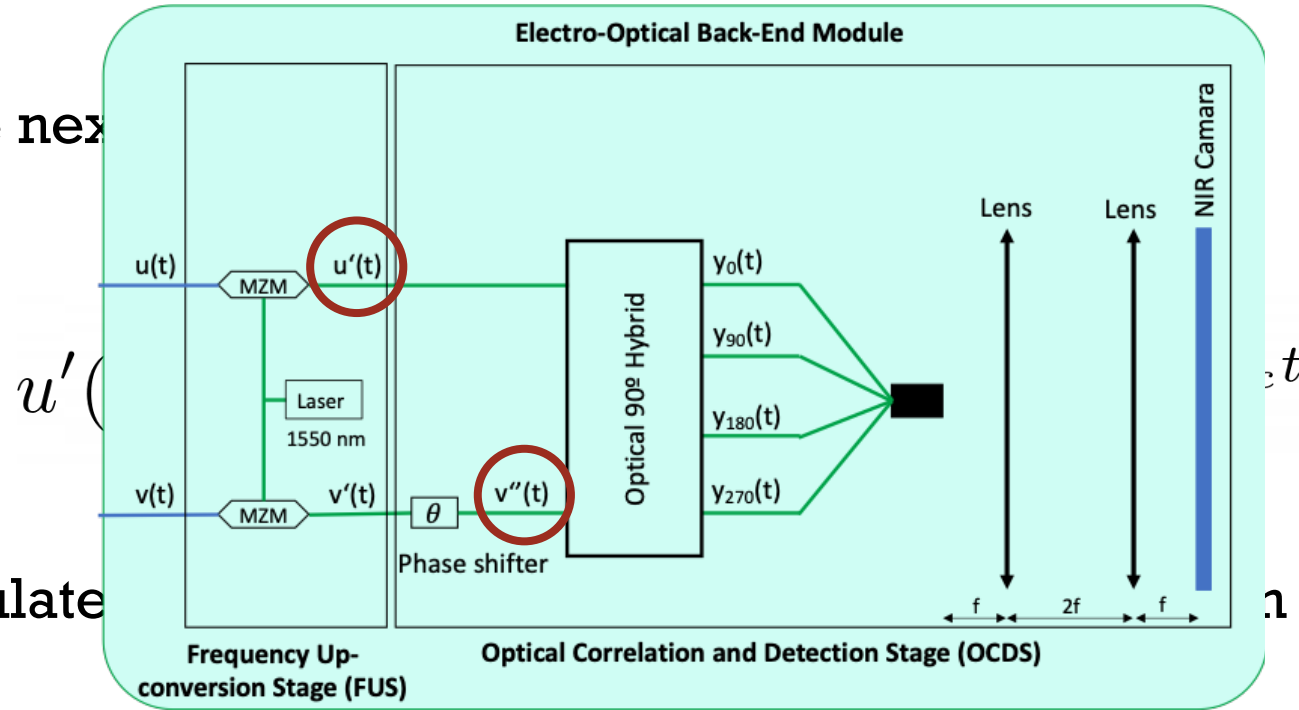


- So our modulated signals, adding also the phase modulation are:

$$\begin{aligned} u'(t) &= \frac{A}{2} \left(e^{i2\pi(f_m + f_c)t} + e^{i2\pi(f_m - f_c)t} \right) e^{i\phi} + k e^{i2\pi f_c t} \\ v''(t) &= \frac{A}{2} \left(e^{i2\pi(f_m + f_c)t} + e^{i2\pi(f_m - f_c)t} \right) i e^{i(\theta(t) - \phi)} + k e^{i2\pi f_c t} e^{i\theta(t)} \end{aligned}$$

THEORETICAL MODEL

- We used the next



- So our modulate

are:

$$\begin{aligned}
 u'(t) &= \frac{A}{2} \left(e^{i2\pi(f_m + f_c)t} + e^{i2\pi(f_m - f_c)t} \right) e^{i\phi} + k e^{i2\pi f_c t} \\
 v''(t) &= \frac{A}{2} \left(e^{i2\pi(f_m + f_c)t} + e^{i2\pi(f_m - f_c)t} \right) i e^{i(\theta(t) - \phi)} + k e^{i2\pi f_c t} e^{i\theta(t)}
 \end{aligned}$$

THEORETICAL MODEL

- The 90° optical Hybrid can be modelled with this equations:

$$\begin{aligned}y_0(t) &= u'(t) + v''(t)e^{-i\pi/2} \\y_{90}(t) &= u'(t)e^{-i\pi/2} + v''(t)e^{-i\pi/2} \\y_{180}(t) &= u'(t)e^{-i\pi/2} + v''(t) \\y_{270}(t) &= u'(t)e^{i\pi} + v''(t)\end{aligned}$$

THEORETICAL MODEL

- The output signals are:

$$y_0(t) = \frac{A}{2} \left(e^{i2\pi(f_m+f_c)t} + e^{i2\pi(f_m-f_c)t} \right) \left(e^{i\phi} + e^{i(\theta(t)-\phi)} \right) + ke^{i2\pi f_c t} \left(1 - ie^{i\theta(t)} \right)$$

$$y_{90}(t) = -\frac{A}{2} \left(e^{i2\pi(f_m+f_c)t} + e^{i2\pi(f_m-f_c)t} \right) \left(e^{i(\theta(t)-\phi)} - ie^{i\phi} \right) - ike^{i2\pi f_c t} \left(1 + e^{i\theta(t)} \right)$$

$$y_{180}(t) = i\frac{A}{2} \left(e^{i2\pi(f_m+f_c)t} + e^{i2\pi(f_m-f_c)t} \right) \left(e^{i(\theta(t)-\phi)} - e^{i\phi} \right) + ke^{i2\pi f_c t} \left(e^{i\theta(t)} - i \right)$$

$$y_{270}(t) = -\frac{A}{2} \left(e^{i2\pi(f_m+f_c)t} + e^{i2\pi(f_m-f_c)t} \right) \left(e^{i\phi} - ie^{i(\theta(t)-\phi)} \right) + ke^{i2\pi f_c t} \left(e^{i\theta(t)} - 1 \right)$$

THEORETICAL MODEL

- Considering $k = 0$, calculating the intensity of the signal ($|y|^2$) and low-pass filtering the laser NIR frequency signals we obtain the next expression:

$$|y_0(t)|^2 = \frac{A^2}{4} (1 + \cos(\theta(t) - 2\phi))$$

$$|y_{90}(t)|^2 = \frac{A^2}{4} (1 + \cos(\theta(t) - (2\phi - \pi/2)))$$

$$|y_{180}(t)|^2 = \frac{A^2}{4} (1 + \cos(\theta(t) - (2\phi - \pi)))$$

$$|y_{270}(t)|^2 = \frac{A^2}{4} (1 + \cos(\theta(t) - (2\phi - 3\pi/2)))$$

- Where:

$$\theta(t) = \nu t + \text{rand}(t)$$

THEORETICAL MODEL

- If ν is much higher than the natural frequency of the noise, we can assume that for the Interval $t^* \in \left[0, 3\frac{1}{\nu}\right]$ the noise can be assumed as constant, leading to:

$$|y_0(t^*)|^2 = \frac{A^2}{4} (1 + \cos(\nu t^* - (2\phi - r)))$$

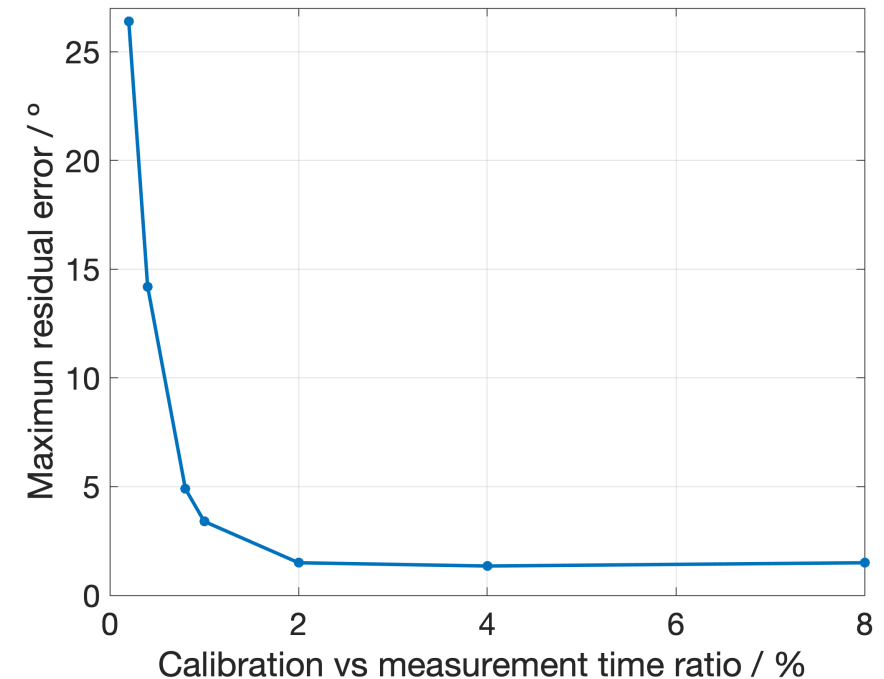
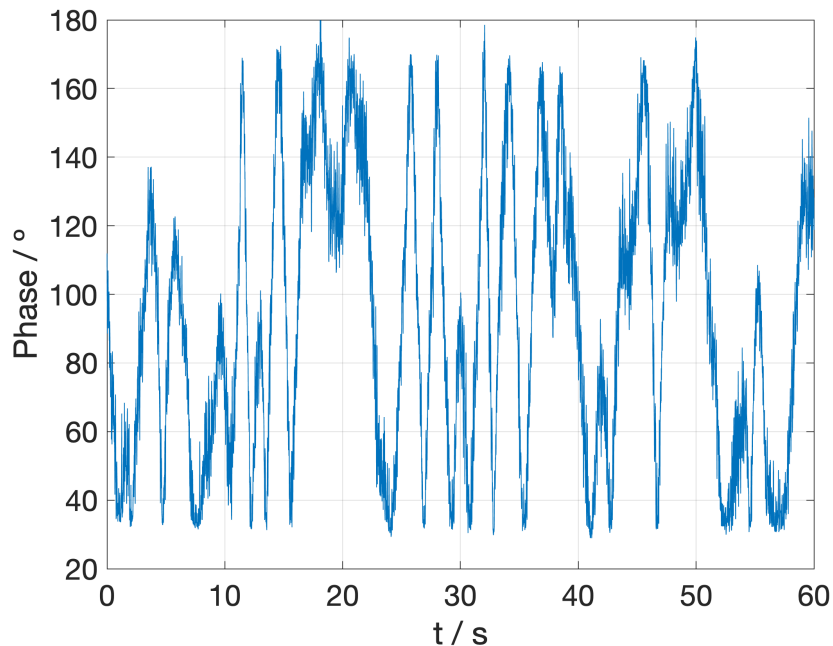
$$|y_{90}(t^*)|^2 = \frac{A^2}{4} (1 + \cos(\nu t^* - (2\phi - \pi/2 - r)))$$

$$|y_{180}(t^*)|^2 = \frac{A^2}{4} (1 + \cos(\nu t^* - (2\phi - \pi - r)))$$

$$|y_{270}(t^*)|^2 = \frac{A^2}{4} (1 + \cos(\nu t^* - (2\phi - 3\pi/2 - r)))$$

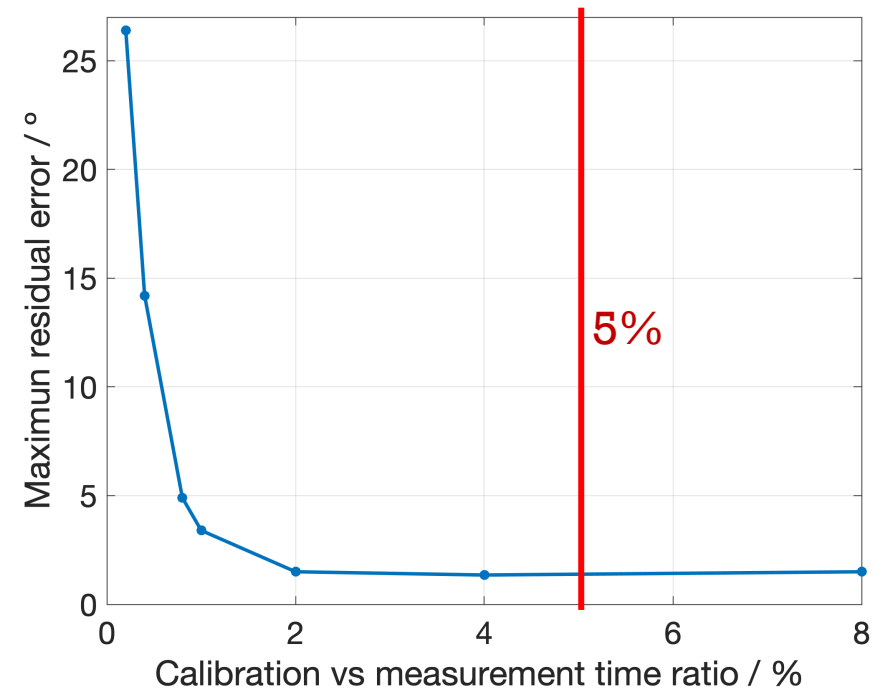
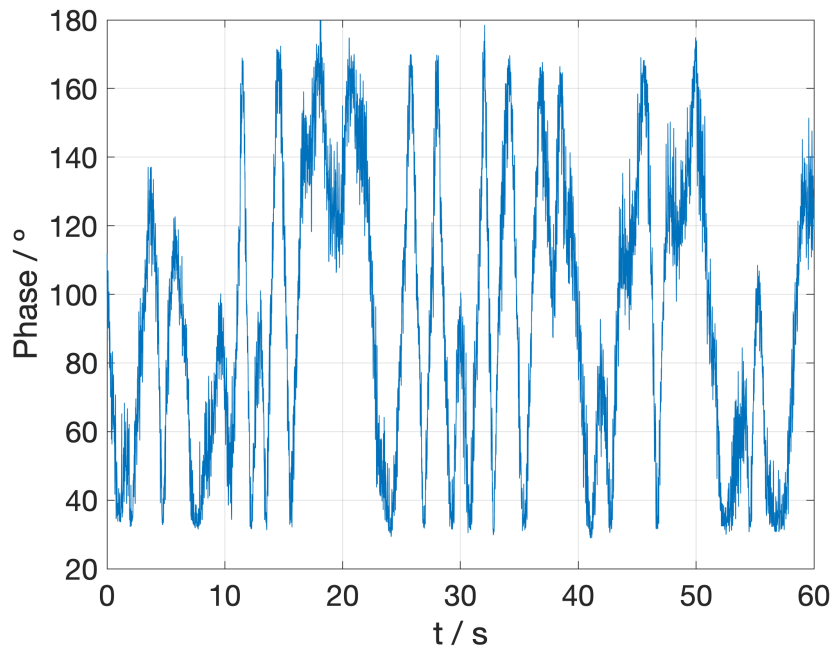
NOISE CALIBRATION

- Obtain the value of the random phase in the system during long time-spaced periods of time by making dark measurements (with no input signal).
- In order to test the method we have made a simulation where the phase modulation frequency is 3 orders of magnitude higher than the natural frequency of the noise (We use the signal measured in the lab)

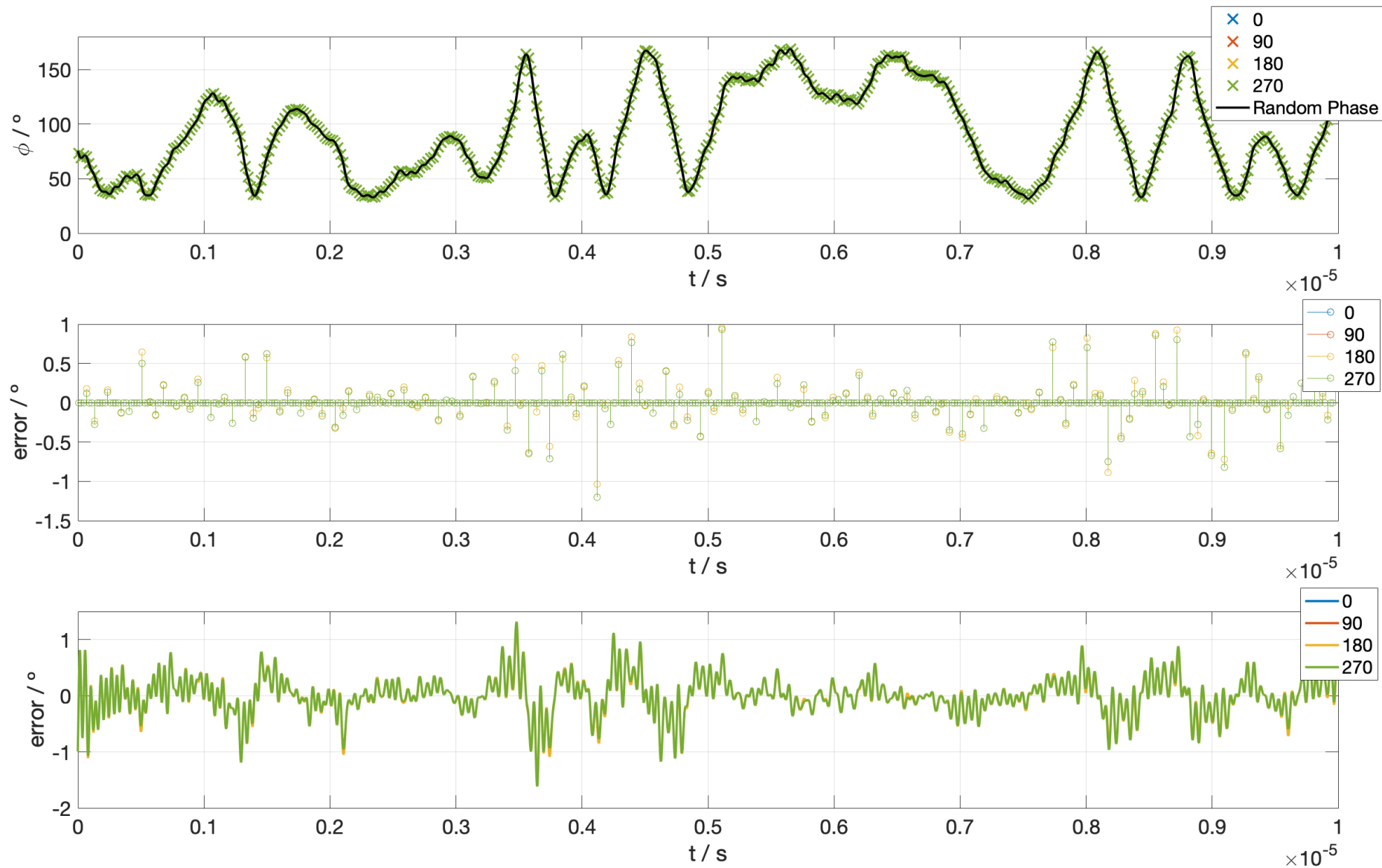


NOISE CALIBRATION

- Obtain the value of the random phase in the system during long time-spaced periods of time by making dark measurements (with no input signal).
- In order to test the method we have made a simulation where the phase modulation frequency is 3 orders of magnitude higher than the natural frequency of the noise (We use the signal measured in the lab)



SIMULATION RESULTS



CONCLUSIONS

- The proposed polarimeter allow us to make both, interferometry and direct detection studies, for the characterization of the synchrotron radiation between 10 and 20 GHz, reducing the complexity of the system
- We have found an important $1/f$ -like noise that prevents us of using the planned phase modulators.
- Even with the system level noise found on the demonstrator, we have proved, by simulations, that it can be partially calibrated in a real experiment without loss of a relevant quantity of observation time.
- Also, the polarimeter can be further optimised by fully integration of the electro-optical part in small chips of InP, which improves its behaviour. PIC design will be presented in a future paper.



CSIC

CONSEJO SUPERIOR DE INVESTIGACIONES CIENTÍFICAS



EXCELENCIA
MARÍA
DE MAEZTU

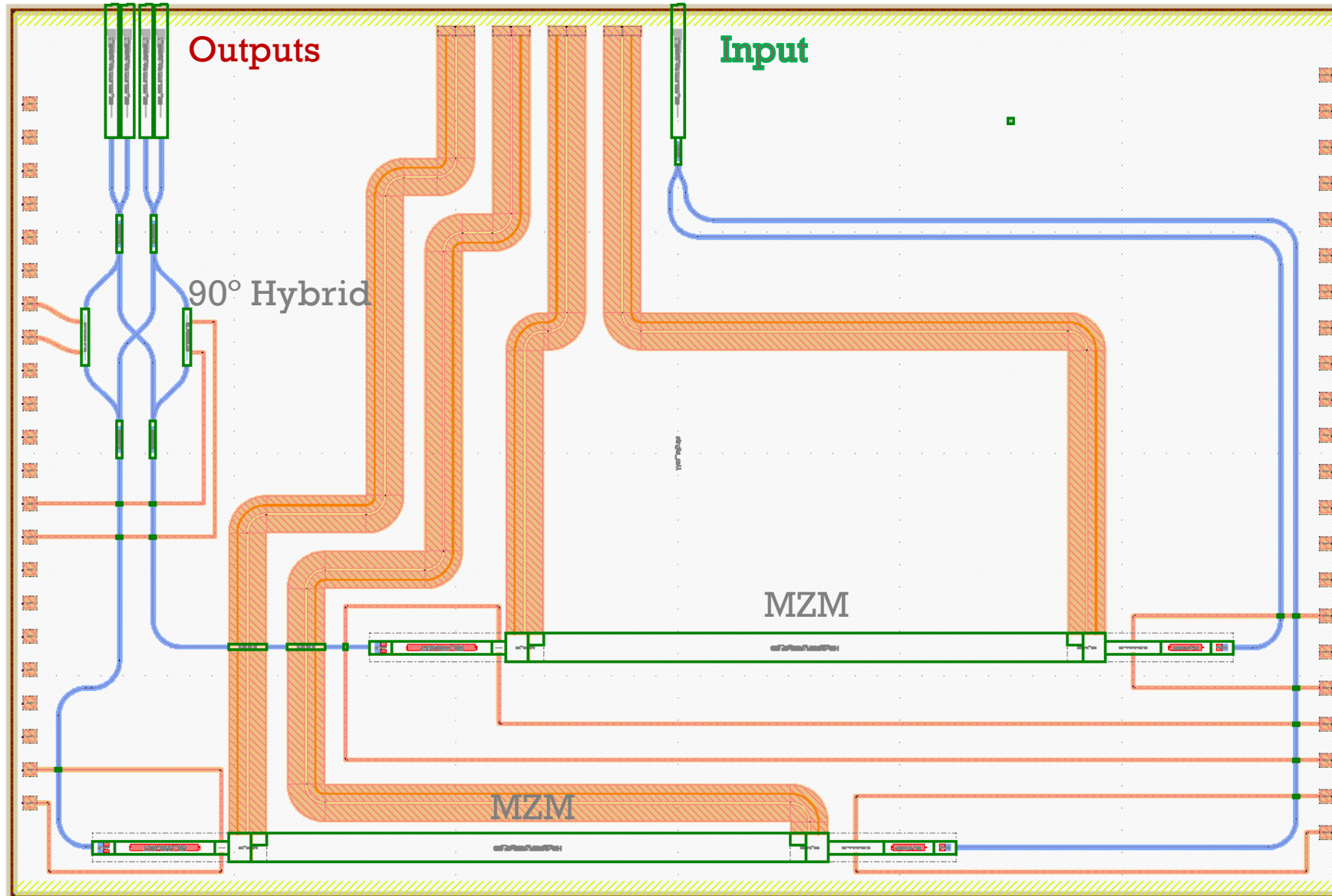


THANK YOU!

G. Pascual-Cisneros, F.J. Casas, P. Vielva



NEW SOLUTION: PICS



8 x 12 mm